Environ Monit Assess (2013) 185:9177–9189
DOI 10.1007/s10661-013-3245-9

Statistical distributions of trace metal concentrations in the northwestern Mediterranean atmospheric aerosol

Thomas Robin · Lionel Guidi · Aurélie Dufour · Christophe Migon

Received: 14 March 2012 / Accepted: 26 April 2013 / Published online: 18 May 2013

Abstract The concentrations of 11 crustal and anthropogenic trace metals (Li, Al, V, Mn, Fe, Co, Ni, Cu, Zn, Cd, Pb) were measured from 2006 to 2008 in the atmospheric aerosol at a northwestern Mediterranean coast (station of Cap Ferrat, situated on the southeastern coast of France). Statistical models (lognormal, Weibull, and gamma) that best represented the trace metal distribution for this environment are described. The lognormal model was selected for the distributions of (in decreasing strength of the fit) Al, Co, Li, Zn, Mn, Cu, Pb, and Cd, i.e., metals that are introduced into the atmospheric aerosol by pulses inducing temporal variability in their concentrations. The gamma model was associated with Fe, i.e., metals that exhibit less inter-annual variability than the former trace metals. The third mode (Weibull) represented the distribution of the concentrations of V and Ni. The statistical approach presented in this study contributed to better define and constrain the distribution of the 11 trace metals of the atmospheric aerosol from the northwestern Mediterranean coast. In a close future, knowledge of these statistical distributions will allow using convolution models to separate their natural and anthropogenic contributions, therefore increasing our ability to study anthropogenic emissions of trace metals and their impact on the environment.

Keywords Trace metals · Probability distribution analysis · Lognormal · Weibull · Gamma · Likelihood maximization

T. Robin (✉)
Transport and Mobility Laboratory, TRANSP-OR Ecole Polytechnique Fédérale de Lausanne,
1015 Lausanne, Switzerland
e-mail: thomas.robin.epfl@gmail.com

L. Guidi
Department of Oceanography, University of Hawaii,
Honolulu, HI 96822, USA

A. Dufour · C. Migon
Université Pierre et Marie Curie (UPMC), UMR 7093,
Observatoire Océanologique de Villefranche-sur-mer,
06234 Villefranche-sur-Mer, France

A. Dufour · C. Migon
CNRS/INSU, UMR 7093,
Laboratoire d'Océanographie de Villefranche,
06234 Villefranche-sur-Mer, France

Introduction

Studies dealing with air pollution or atmospheric deposition on natural surfaces require a good knowledge of the statistical behavior of airborne elemental concentrations. The concentration of trace metals (TMs) in the atmospheric aerosol is generally assumed to be the combined result of land-based emissions and stochastic processes like climatic and meteorological conditions that govern atmospheric transport (e.g., Morel et al. 1999). Trace metal concentrations in the

atmospheric aerosol are inherently random variables, and their temporal variations result from stochastic emission events from various independent sources. Therefore, their statistical distributions are the product of a variety of complex processes that are difficult to model and predict with accuracy. Determination of the proper distribution of elemental concentrations in the aerosol allows knowing which type of mean and standard deviation best fit to describe aerosol dynamics (Blackwood 1991). Knowledge of the concentration distribution helps to assess the impact of extreme events on the mean concentration values and time lag between extreme events (Georgopoulos and Seinfeld 1982) or to formulate steady hypothesis in deconvolution studies (Migon and Caccia 1990). More generally, this contributes to advance knowledge of the origin, magnitude, and variability of elemental concentrations in the aerosol. This is particularly important for the case of atmospherically transported TMs because of their environmental and biogeochemical significance. Knowledge of the nature of land-based emission sources (e.g., natural versus anthropogenic), the effects of transport processes, the understanding of correlations, etc., are based upon statistical analysis of aerosol data sets, which requires the specification of their underlying distributions.

Lognormal distribution is the most common choice to describe environmental data (Blackwood 1992; Georgiadis et al. 1998). However, in studies dealing with the dynamics of atmospheric aerosol in non-urban coastal environments, the low frequency of sample acquisition, combined with the long sampling duration, often results in little discriminating power. Standard sampling protocols are generally used in order to obtain results which could be compared with the literature (Rumburg et al. 2001).

Although Ott (1990) argued that the successive random dilution of pollutants in the atmosphere explains why pollutant concentrations fit a lognormal distribution, Bencala and Seinfeld (1976) had previously shown that other distributions can describe pollutant concentrations in the atmospheric aerosol. The present work aims to describe the models that best fit the distribution of the concentrations of 11 TMs (Li, Al, V, Mn, Fe, Co, Ni, Cu, Zn, Cd, Pb) for the northwestern Mediterranean coastal environments. The lognormal, Weibull, and gamma models are evaluated using log-likelihood maximization.

Material and methods

Sampling

Atmospheric aerosol was continuously sampled at the Cap Ferrat naval signal station, situated on the south-eastern coast of France (43°41′ N, 7°19′30″ E; altitude, 130 m; Fig. 1) in 2006, 2007, and 2008. This sampling site is not affected by local sea spray or local contamination, as shown elsewhere (Sandroni and Migon 1997; Guieu et al. 1997; Chester et al. 1997). Saharan events are episodically superimposed to homogeneous anthropogenic influences, mainly in the spring and, to a lesser extent, summer (Marticorena and Bergametti 1996). Aerosol was sampled at the top of a 6-m-high mast by pumping air through cellulose acetate filters (porosity, 0.45 μm; diameter, 47 mm; Sartorius SM 11106). The mean pumping rate was 25 ± 1 m^3 day^{-1} during approximately 1 week, for a mean air volume of 175 m^3. Atmospheric aerosol was monitored from 2006 to 2008.

Total suspended particles were sampled instead of particles <10 μm in diameter (Fang et al. 2010; Kim et al. 2006) for two reasons: (1) The definition of statistical models that best fit the concentrations of TMs in the atmospheric aerosol requires large data sets, i.e., time series that includes samples collected when the use of PM_{10} was not generalized in Europe, and (2) this study does not deal with particle size distributions; it aims to describe the concentration distributions of all the particles that reach the northwestern Mediterranean coastal troposphere, including coarse (>10 μm) particles from, e.g., Saharan dust emissions.

Sample mineralization and analysis

Samples were dissolved by acid treatment as well as blank filters and two standard reference materials (SRMs). Each filter was folded into four and introduced into an acid cleaned Teflon vial (7 mL) in which 1 mL HNO_3 (65 %) was added. The vial was closed and put into a larger Teflon vial (60 mL) and left at room temperature until complete dissolution of the membrane. Then, the apparatus was kept tightly closed for 12 h in an oven at 150 °C. Vials were then cooled in a laminar airflow hood and left open until the red smoke had evolved (which indicates that all HNO_3 has evaporated). The remainder was dissolved

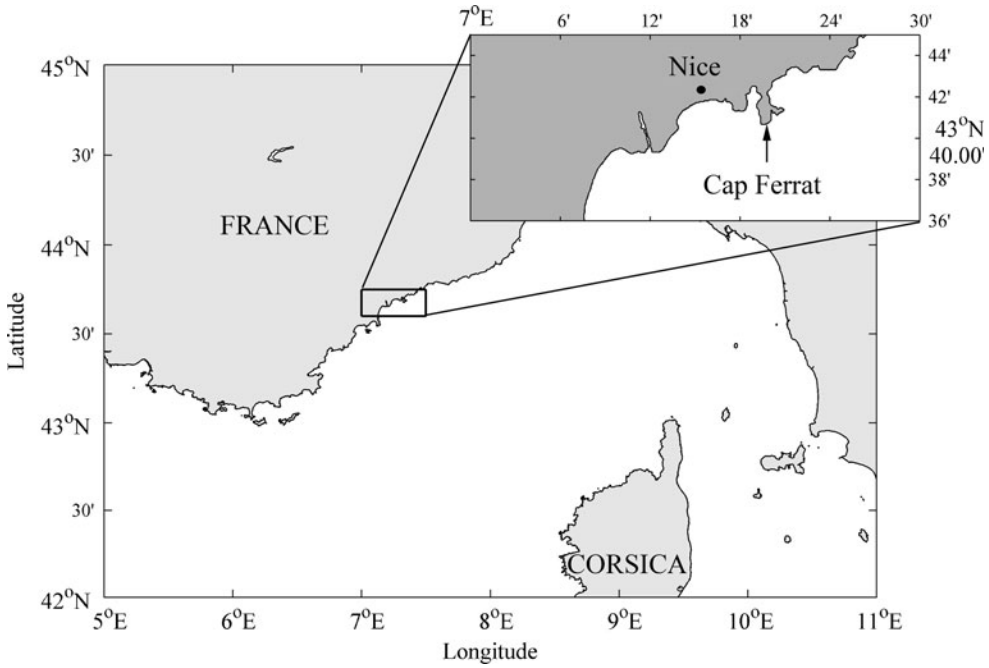

Fig. 1 Location of the Cap Ferrat coastal sampling station

again with 500 μL HNO_3 (14 M) and 300 μL HF (23 M) and left for 24 h (without evaporation) prior to being stored again in a drying oven for 12 h. A white residue was obtained and dissolved in 1 mL HNO_3 (1 M), ultrasonically agitated for 2 h, and made up to 9 mL with Milli-Q water. The solution was finally stored in an acid-cleaned polypropylene vial (10 mL) until analysis. All reagents were Suprapur® grade, provided by Merck (Darmstadt, Germany). All analyses were carried out under laminar airflow benches in a class 100 clean room. This mineralization procedure has been previously validated using different analytical techniques on SRMs (Heimbürger et al. 2010).

Two analytical techniques were used: Inductively coupled plasma atomic emission spectroscopy (ICP-AES) was used for Al and Fe and inductively coupled mass spectrometry (ICP-MS) was used for Cd, Co, Cu, Li, Mn, Ni, Pb, V, and Zn. Measurements by ICP-AES were performed with a Jobin-Yvon JY 138 S Ultrace analyzer. Measurements by ICP-MS were performed with a Thermo Elemental ×7 device. For each TM, the analytical methods, detection limits, and the concentrations of blank filters compared with the aerosol concentration range are given in Table 1. The analytical procedures (mineralization and analysis) were regularly checked using two SRMs (MESS-2 from the National Research Council, Ottawa, Canada, and NIST-2783 Air particulate on filter media from the National Institute of Standards & Technology). The results were always within the quoted confidence intervals given for the SRMs (Table 1). The concentration values of blank filters were low (always <10 %) when compared with the aerosol concentration range. Additional analytical details can be found in Migon et al. (2000) and Chiffoleau et al. (2004).

Data processing and time series reconstruction

Aerosol samples were not collected at a constant time rate; therefore, raw data are difficult to study with standard time series or distribution analysis. Trace metal concentrations were measured in nanograms per liter approximately weekly. The numbers of samples for 2006, 2007, and 2008 are 37, 35, and 47, respectively, representing 30 % of the 3 years. In order to solve this issue, data were concentrated into one single year (called aggregated year) to study intra-annual trends. This can be done after ensuring that yearly distributions are similar. Therefore, we normalized each year of all time series by the median of the 3 years combined. After this step, all TM yearly distributions were tested as not significantly different (Kruskal–Wallis: $p<0.001$). The concentrations were then averaged for multiple measurements of a single day of the aggregated year. Missing values of the

Table 1 Analytical methods, detection limits, concentration of blank filters (expressed as percentage of the aerosol concentration range), and certified and measured levels of SRM, expressed in milligrams per kilogram (MESS-2) and in nanograms (NIST-2783)

TM	Analytical method	Detection limit (ng L^{-1})	Contribution of blank (%)	SRM MESS-2 (certified)	SRM MESS-2 (measured)	SRM NIST (certified)	SRM NIST (measured)
Al	ICP-AES	1500	0.03–2.9			23,210±530	22,990±90
Fe	ICP-AES	600	0.02–0.6			26,500±1,600	26,700±450
Li	ICP-MS	1	0.14–6.0	73.9±0.7	74.4±0.5		
Mn	ICP-MS	5	0.06–2.16	365±21	355±6	320±12	319±4
Co	ICP-MS	1	0.16–5.5	13.8±1.4	12.5±1.0	7.7±1.2	7.0±0.8
Ni	ICP-MS	8	0.53–9.4	49.3±1.8	50.1±0.3	68±12	68±4
V	ICP-MS	21	0.03–0.05	252±10	248±7	48.5±6.0	45.4±4.5
Cu	ICP-MS	5	0.27–3.5	39.3±2.0	38.0±1.2	404±42	388±15
Pb	ICP-MS	2	0.09–2.4	21.9±1.2	22.9±0.8	317±54	331±30
Cd	ICP-MS	1	0.19–2.5	0.24±0.01	0.24±0.01		
Zn	ICP-MS	9	0.08–1.06	172±16	185±10	1790±130	1820±50

aggregated year were then predicted using a cubic polynomial interpolation for each TM. Because of the original time series sampling date and to avoid extrapolation, we were limited to a reconstructed year of 356 days instead of 365. However, this limitation is of little impact on the estimation of TM concentration distributions since it only represents a cut of 2.5 % of a full year. The reconstructed annual time series was sampled at a constant time rate of a day over 3. The sampling rate was chosen in order to be consistent with the data collection. Sampled data correspond to 119 concentrations for each TM equal to the total number of raw measurements for the 3 years. Finally, all concentrations were normalized by their respective maximum, leading to values ranging from 0 to 1 in order to allow TM comparisons.

Stable conditions of element concentrations

Trace metal concentrations should follow constant statistical properties (i.e., should be controlled by stationary processes) in order to study their statistical properties using probability density functions (PDFs). A stationary process is a stochastic process whose joint probability distribution does not change when shifted in time or space (the space cannot interfere here as there is a unique location). Consequently, we check that there is no or limited temporal relationship between TM concentrations. The stationarity of each TM was verified looking at their autocorrelation function. The autocorrelation between Y_t and Y_s (at time t and s, respectively) of a random variable Y is defined as follows:

$$R(t-s) = \frac{E[(Y_t - E(Y))(Y_s - E(Y))]}{\sqrt{E(Y - E(Y))^2}} \quad (1)$$

where E stands for the statistical Esperance. $R(t-s)$ is included in [−1,1]: 1 means that Y_t and Y_s are perfectly correlated, −1 means they are perfectly anti-correlated, and 0 means they are uncorrelated. Pearson's estimator was used to calculate the autocorrelation according to

$$R(p) = \frac{1}{(n-p)E\left((Y - E(Y))^2\right)} \times \sum_{i=1}^{n-p} (Y_i - E(Y))\left(Y_{i+p} - E(Y)\right) \quad (2)$$

where p represents the number of days between two measurements and n corresponds to the total number of days considered in the aggregated year. Autocorrelations were computed for p ranging between 0 and 356 days. Pearson's correlation coefficient is chosen as it is the most standard to detect linear relationships.

Trace metal models in the atmospheric aerosol

The characterization of the distributions of the TM concentrations requires a set of PDFs that are likely to represent the aerosol concentrations. In the following,

the term "model" refers to a specific statistical probability distribution. Based on the literature review, three models (lognormal, gamma, and Weibull) were selected (e.g., Georgiadis et al. 1998; Taylor et al. 1986; Bencala and Seinfeld 1976; Georgopoulos and Seinfeld 1982) and their associated PDF and parameters estimated.

The lognormal model assumes that the logarithm of the considered variable is normal. This model can only be applied to a variable that is a multiplicative product of many independent, random, and positive variables, which is the case for TM emissions. Its associated PDF is a function of two parameters, μ and σ:

$$f(x) = \frac{1}{\sqrt{2\pi}\sigma x} \exp\left(\frac{(\log(x) - \mu)^2}{2\sigma^2}\right) \quad (3)$$

The gamma model is designed for random variables that are the sum of independent random variables following exponential probability models. The advantage of this model is that it has a less heavy right tail, which lowers the weight of extreme events. Its PDF is a function of two parameters, $\theta > 0, k > 0$.

$$f(x) = \frac{1}{\Gamma(k)\theta}\left(\frac{x}{\theta}\right)^{k-1} \exp\left(-\frac{x}{\theta}\right) \quad (4)$$

Γ refers to the standard gamma function, which is a function of the first parameter of the gamma model, k.

$$\Gamma(k) = \int_0^{+\infty} t^{k-1} e^{-t}\, dt \quad (5)$$

where t is an integration variable.

For the Weibull model, the PDF is a function of $\lambda > 0, \eta > 0$.

$$f(x) = \frac{\lambda}{\eta}\left(\frac{x}{\eta}\right)^{\lambda-1} \exp\left(-\left(\frac{x}{\eta}\right)^{\lambda}\right) \quad (6)$$

This model is flexible in a mathematical sense because it can simulate the behavior of other models depending on the value of its first parameter λ, such as the normal (large value for λ) and the exponential ($\lambda \leq 1$). The density form is more symmetric than in the lognormal and gamma cases.

For each element, we used a log-likelihood maximization ($L_{i,d}$) method to estimate the parameters of each model. It consists in maximizing the following function:

$$L_{i,d}(\beta_{i,d}) = \prod_{t=1}^{119} \log\left(f_d(x_{i,t}/\beta_{i,d})\right) \quad (7)$$

where i represents the TM; d the model (lognormal, Weibull, or gamma); t the date of measurement; f_d the PDF of d; $x_{i,t}$ the measurement of the concentration of the TM i at time t; and $\beta_{i,d}$ the vector of parameters associated with the model d for the TM i. Note that the three considered models have two parameters; therefore, the size of $\beta_{i,d}$ is 2. d=1 corresponds to the lognormal model $\beta_{i,1} = (\mu_i, \sigma_i)$; d=2 to the Weibull model $\beta_{i,2} = (\lambda_i, \eta_i)$; and d=3 to the gamma model $\beta_{i,3} = (\theta_i, k_i)$.

The likelihood function depends on the model parameters and can be interpreted as the probability of obtaining the actually observed TM concentrations, assuming that the TM concentration follows the given model.

Analysis of the impact of extreme values on model adjustments

For each TM, an extreme value (EV) is defined as a TM concentration larger than the mean concentration plus 2 standard deviations. After removing EVs to the TM time series, the remaining signal was analyzed in order to test the robustness of the models, and the little influence of the EVs on the adjustment of these models to the distribution of the TM concentrations. However, the number of values describing the series with EVs and without EVs is different, preventing direct comparison of the adjustments.

Results and discussion

Trace metal model selection

Raw TM concentrations can be found online (ftp://oceane.obs-vlfr.fr/pub/migon). The autocorrelation functions for all TMs are presented in Fig. 2. The sharp decrease of the autocorrelation function indicates that the TMs are not time-dependent (the autocorrelation function rapidly crosses the 95 %

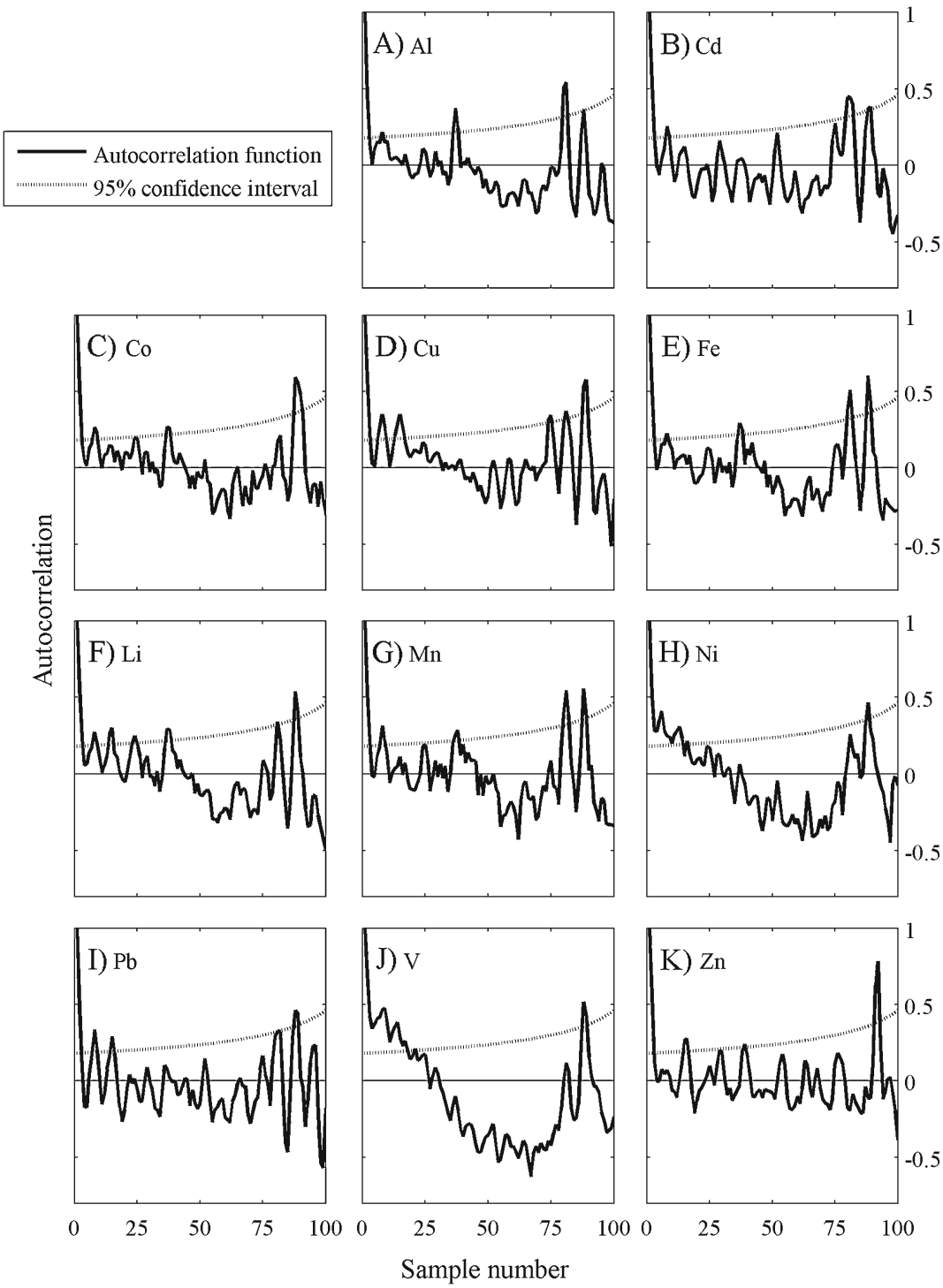

Fig. 2 Autocorrelations of the TM signals

confidence interval). The log-likelihood maximization of the couple of parameters of each model has been calculated using Matlab software (The Mathworks, Inc., Natick, MA, USA). Parameters are displayed in Table 2 for the three models. Note that for each parameter, lower and upper bounds of the confidence

Table 2 Estimated parameters of the three models (lognormal, Weibull, and gamma) with STD being the confidence interval at 95 % with the lower and upper bounds

TM	Lognormal		Weibull		Gamma	
	μ_i (STD)	σ_i (STD)	λ_i (STD)	η_i (STD)	θ_i (STD)	k_i (STD)
Li	−1.94 (−2.06 to −1.82)	0.66 (0.58–0.75)	1.44 (1.27–1.63)	0.20 (0.18–0.23)	2.36 (1.86–3.00)	0.08 (0.06–0.10)
Al	−2.42 (−2.57 to −2.26)	0.83 (0.74–0.95)	1.11 (0.98–1.26)	0.14 (0.12–0.16)	1.46 (1.16–1.84)	0.09 (0.07–0.12)
V	−1.55 (−1.70 to −1.41)	0.80 (0.71–0.92)	1.51 (1.31–1.74)	0.31 (0.27–0.35)	2.01 (1.59–2.55)	0.14 (0.10–0.18)
Mn	−1.75 (−1.87 to −1.64)	0.64 (0.56–0.73)	1.54 (1.36–1.75)	0.24 (0.21–0.27)	2.61 (2.05–3.31)	0.08 (0.06–0.11)
Fe	−1.97 (−2.10 to −1.84)	0.73 (0.65–0.84)	1.41 (1.25–1.60)	0.20 (0.17–0.23)	2.17 (1.71–2.75)	0.08 (0.06–0.11)
Co	−1.79 (−1.89 to −1.69)	0.56 (0.50–0.65)	1.63 (1.45–1.84)	0.22 (0.20–0.25)	3.15 (2.47–4.01)	0.06 (0.05–0.08)
Ni	−1.50 (−1.74 to −1.26)	1.30 (1.16–1.49)	1.60 (1.39–1.84)	0.33 (0.29–0.37)	1.89 (1.49–2.39)	0.16 (0.12–0.21)
Cu	−1.15 (−1.23 to −1.07)	0.43 (0.38–0.49)	2.30 (2.02–2.61)	0.39 (0.36–0.43)	5.50 (4.30–7.04)	0.06 (0.05–0.08)
Zn	−2.08 (−2.23 to −1.94)	0.79 (0.70–0.91)	1.24 (1.09–1.40)	0.18 (0.16–0.22)	1.72 (1.36–2.18)	0.10 (0.08–0.13)
Cd	−1.31 (−1.40 to −1.21)	0.54 (0.48–0.62)	1.87 (1.65–2.13)	0.35 (0.32–0.39)	3.60 (2.82–4.59)	0.09 (0.07–0.11)
Pb	−1.24 (−1.33 to −1.14)	0.50 (0.45–0.58)	1.96 (1.72–2.23)	0.38 (0.34–0.41)	4.02 (3.15–5.14)	0.08 (0.06–0.11)

interval at the 95 % level are given. Log-likelihood values are presented in Table 3.

For each element, one has to choose the model with the best fit to the observed distributions of TM concentrations. The Akaike information criteria (AIC; Akaike 1974) and Bayesian information criteria (BIC; Schwarz 1978) are well adapted to deal with such issues. They are tools commonly used for parametric model selection. However, because the three models have equal numbers of parameters and TMs have the same sample frequency, computing the AIC or BIC is equivalent to comparing directly $L_{i,d}(\beta_{i,d})$. Therefore, the model that best fits a given TM distribution is the one with the highest log-likelihood (Table 3). In addition, data have been normalized, allowing direct comparison among TMs. Trace metals can then be ordered in a function of the goodness of the adjustment of the model to the data (Table 4). The lognormal model was well adapted to most TMs (Al, Co, Li, Zn, Fe, Mn, Cu, Pb, and Cd), while the gamma model was selected for V and the Weibull model for Ni. However, when EVs are removed from the original time series, model selections are slightly modified. Fe changed from lognormal to gamma, while V becomes Weibull. The adjustments of the models are presented in Fig. 3. Each subplot includes the observed probability distribution compared with the three models. In most cases, the lognormal model well fitted the TM distributions. In addition, the heavy right tail of the lognormal model accounted

Table 3 Estimated log-likelihoods for each element and each model, with and without EVs

TM	$L_{i,1}(\beta_{i,1})$ with EVs/without EVs	$L_{i,2}(\beta_{i,2})$ with EVs/without EVs	$L_{i,3}(\beta_{i,3})$ with EVs/without EVs
Li	112.37/117.43	97.80/106.18	104.76/112.51
Al	141.22/146.38	124.44/131.96	127.76/135.88
V	43.16/45.79	47.91/51.88	48.15/51.55
Mn	94.11/98.54	82.89/90.17	89.36/95.85
Fe	103.12/107.50	97.60/105.81	102.55/109.82
Co	112.52/118.16	96.42/106.66	105.93/114.66
Ni	−21.30/−19.44	42.25/46.18	37.15/40.03
Cu	68.40/75.86	57.23/70.06	65.67/75.24
Zn	107.30/111.57	96.07/102.35	100.25/106.63
Cd	60.32/63.65	50.81/55.51	57.28/61.45
Pb	60.57/63.93	48.48/53.02	56.10/60.19

$L_{i,1}(\beta_{i,1})$ corresponds to the lognormal model, $L_{i,2}(\beta_{i,2})$ to the Weibull model, and $L_{i,3}(\beta_{i,3})$ to the gamma model

Table 4 Selection of the model for each element following the strength of the fit decreasing from the first to the last

Model	TMs (with EVs)	TMs (without EVs)
Lognormal	Al, Co, Li, Zn, Fe, Mn, Cu, Pb, Cd	Al, Co, Li, Zn, Mn, Cu, Pb, Cd
Weibull	Ni	V, Ni
Gamma	V	Fe

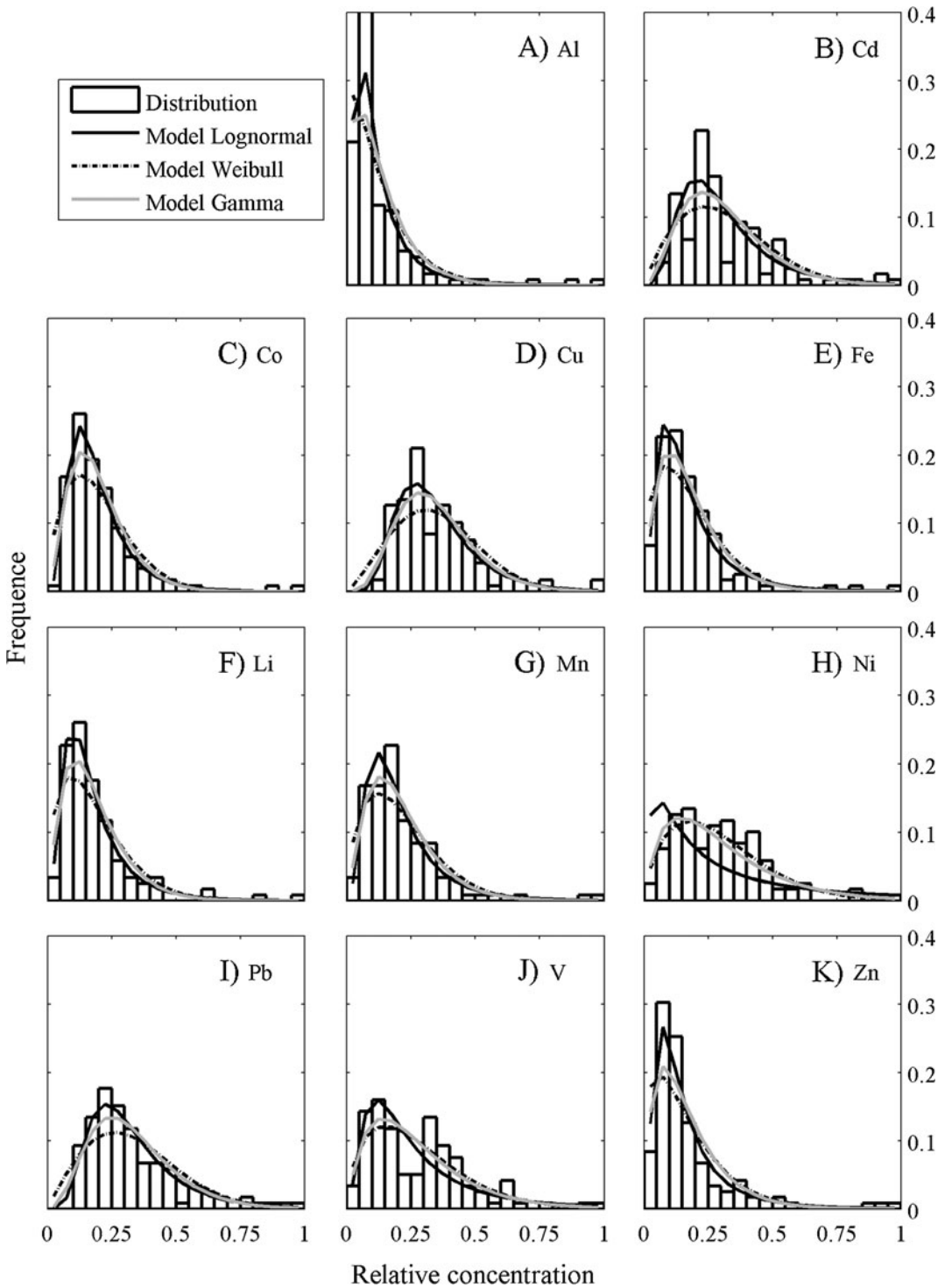

Fig. 3 Distributions of the TMs and models adjusted

well for the measurements of high concentrations. The gamma model was more adapted to the TM distributions that were bimodal. This important result suggests that the observed concentration distribution of these TMs was a combination of at least two independent signals with different modal distributions.

Table 4 summarizes the models that were associated with the TM distributions. Trace metals following a lognormal distribution can be clustered into two groups: crustal TMs (Al, Co, Li, Mn) and anthropogenic TMs (Pb, Cd, Cu, and Zn). Emissions of crustal TMs are typically associated with Saharan dust events, which are characterized by pulsed emissions (Bonnet and Guieu 2006; Guerzoni et al. 1999). Among anthropogenic TMs, the peculiarity of Pb, Cd, and Zn lies in their inter-annual variability. The inter-annual variability of Pb, Cd, and Zn has been previously evidenced by the analysis of longer time series at the same site, including the period considered here (Heimbürger et al., 2010), which showed decreasing trends in the concentrations of these TMs in the atmospheric aerosol. The steep decrease of Pb concentrations in the environment after the second half of the 1980s was due to the progressive phasing out of leaded gasoline (Flament et al. 1996; Migon et al. 1993). This decrease was still going on by ~75 % between 1995 and 2005 (Migon et al. 2008). More recently, significant changes occurred in Cd and Zn emissions. Improvements resulting from anti-pollution policies in industrial sectors (iron and steel industry, non-ferrous smelters) and in household waste incineration yielded a decrease of Cd emissions by 80 % over the last 40 years in Europe (Pacyna et al. 2009). As well, Zn emissions were reduced because of technical improvements in electric furnace steel plants and standards of household waste incineration. Decreases by ~65 % for Cd and by >50 % for Zn were actually observed between the end of the 1990s and the present time at the Cap Ferrat sampling station (Heimbürger et al. 2010). In addition, Zn is a tracer of urban emission sources, and episodic emissions from the large urban area that borders the northern shores of the Ligurian Sea are likely to give off amounts (i.e., extreme anthropogenic events) of Zn (Wiesner et al. 1998). The combination of Zn temporal evolution and its pulsed behavior might explain the best fit of Zn concentrations with the lognormal model. To various extents, this also applies to Pb and Cd: Pulsed emissions coming from the highly urbanized shore probably contribute to the observed inter-annual variations of Pb and Cd airborne concentrations. Overall, the lognormal model presumably well describes TMs associated with pulsed emissions (e.g., crustal TMs and evolving anthropogenic TMs). Therefore, the "lognormal group" gathers TMs that are introduced into the atmospheric aerosol by pulses with more or less temporal variability in concentrations. For the case of Pb, another specificity might contribute to its bimodal pattern, although this metal does not belong to the "gamma group." It is now admitted that automotive emissions of Pb are close to zero in Western Europe (Migon et al. 2008). The bimodal character of the distribution of Pb concentrations suggests that two distinct populations of Pb loads may be identified in the NW Mediterranean atmosphere: automotive Pb originating from the East and carried by long-range atmospheric transport from North Africa, Middle East, or Eastern Europe (Pirrone et al. 1999), and non-automotive Pb, which presumably originates from industrial regions, e.g., mining activities in Poland or Kazakhstan (Bollhöfer and Rosman 2001), or the iron and steel industry, which represents, e.g., up to more than 40 % of anthropogenic Pb emissions in France (CITEPA 2009).

When EVs are taken into account, Fe belongs to the lognormal group. This presumably results from the prevailing importance of some pulsed Saharan dust inputs that bring very significant amounts of crustal Fe in the atmospheric aerosol. For example, Bonnet and Guieu (2006) attributed up to 99 % of the total 2004 flux of total atmospheric Fe at Cap Ferrat to a few strong pulses of Saharan dust events. Once EVs are removed, they do not mask any more the significance of the anthropogenic component of Fe atmospheric inputs (Migon et al. 2000). This component then appears and Fe follows the gamma model. As a consequence, the temporal variability of Fe aerosol concentrations is lowered due to the removal of EVs (i.e., pulsed Saharan episodes) that are responsible for the great variability, in particular the inter-annual variability (Marticorena and Bergametti 1996).

However, the main feature of the gamma group may be the bimodal concentration pattern, which results, for the case of Fe, from the removal of a prevailing component that previously masked another component. Interestingly, the bimodal pattern is well known for particle size distributions (e.g., Chrysikou and Samara 2009; Venkataraman et al. 1999) and generally mirrors two distinct size groups (fine versus coarse particles), particularly when the atmospheric aerosol is affected by both anthropogenic and natural emission sources (Salma et al. 2002). Seasonal patterns clearly show that Fe aerosol concentrations are composed of two distinct populations resulting from two distinct seasonal atmospheric pathways: On the one hand, crustal Fe is transported by Saharan dust episodes

that generally (but not always) occur in spring and summer (Moulin et al. 1997). On the other hand, anthropogenic Fe is probably transported by northern and northeastern anthropogenic inputs, which are generally observed in winter, in agreement with the transport of European polluted air masses described by Duncan and Bey (2004). Reproducible and significant peaks are also observed at the end of summer/beginning of autumn. These anthropogenic concentrations presumably result from autumnal equinox changes, when the polar front moves to the south, yielding the transport of polluted air masses from northern and northeastern Europe to the western Mediterranean Sea. Barnaba and Gobbi (2004) have used satellite data to suggest that the Ligurian Sea may be more affected by anthropogenic air masses in the autumn than in the winter. This has been observed at the Cap Ferrat sampling site for the case of Pb (Migon et al. 2008). Therefore, these two different atmospheric transport pathways may explain the succession of distinct Fe concentration peaks (i.e., the Fe bimodal pattern) in the Ligurian atmospheric aerosol.

Vanadium belongs to the gamma group when EVs are taken into account (Table 4). Long-range atmospheric transport is supposedly responsible for V inputs from both geogenic and anthropogenic emission sources, hence its bimodal distribution and its belonging to the gamma group: At global scale, anthropogenic sources of V slightly exceed natural ones (Hope 1994), oil combustion being among the most significant anthropogenic contributions (Chiffoleau et al. 2004). However, the most significant concentrations of V seem associated with geogenic influences, as suggested in Fig. 4: The highest V concentration peaks are associated with episodes of the highest Al concentration, i.e., Saharan events. Without EVs, V joins the Weibull group. The Weibull model seems more suitable to represent distributions close to the lognormal model (Aleksandrapoulou et al. 2012), i.e., close to the unimodal pattern (Lu 2003). It is hypothesized that, after the removal of extreme concentrations of V, which result from the occurrence of Saharan dust episodes, one of the contributions (most likely the anthropogenic one) prevails upon the other. Besides, Mijic et al. (2012) have suggested that the Weibull distribution might reflect, for the case of atmospherically transported TMs, a strong influence of transport processes. This is in agreement, at the Cap Ferrat sampling station, with V of which the emission sources (Saharan dust and anthropogenic derived from shipping) are far from the coastal receptor site.

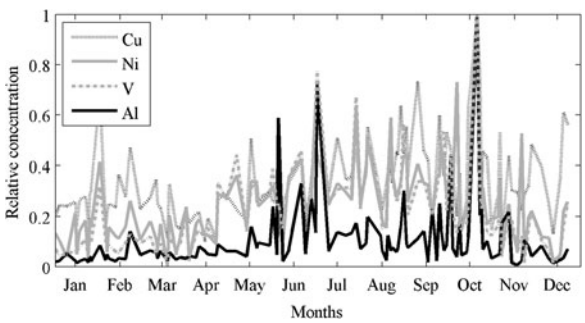

Fig. 4 Seasonal patterns of Cu, Ni, and V aerosol relative concentrations compared to Al

This also applies to Ni, which belongs to the Weibull group, with and without EVs. The main sources of Ni are comparable with those of V, i.e., both geogenic and anthropogenic. On the one hand, Chester et al. (1984) have pointed out relatively low Ni enrichment factors normalized to Al in the northwestern Mediterranean aerosol, suggesting that Ni can be found in geogenic material. The Ligurian region might also be affected by a disused open chrysotile asbestos mine, operating until 1965 near the village of Canari (northeastern Corsica), which still generates Ni-rich waste (Andral et al. 2004). On the other hand, major emissions of anthropogenic Ni affect the whole Mediterranean Sea (Pirrone et al. 1999), and Ridame et al. (1999) have stated that the non-terrigenous fraction of atmospherically deposited Ni varies between 58 and 89 % in the northwestern Mediterranean basin. Moreover, it is known that oil combustion is responsible for the spreading of significant amounts of Ni (Anwari et al. 1992). Indeed, high concentrations are mainly observed between May and November (Fig. 4), i.e., when cruising and pleasure ships frequent northwestern Mediterranean waters. More generally, combustion processes generate particulate anthropogenic TMs, including Ni (Xie et al. 2005; Caggiano et al. 2011). Despite the coexistence of two distinct emission sources of Ni, it is believed that the anthropogenic source prevails upon the geogenic one, leading to a lognormal-like pattern.

Note that seasonal effects are not involved in the model fitting, but can be used to explain the form of the observed TM distributions. Data sets of anthropogenic TMs collected in the atmospheric aerosol with higher frequency hourly or daily (e.g., Georgiadis et al. 1998; Georgopoulos and Seinfeld 1982) necessarily

exhibit a higher variability and, therefore, better fit the lognormal model. Rumburg et al. (2001) have discussed the impact of sampling frequency on the model and found that sampling frequency affects the robustness of the adjustment of the model to the data. Indeed, the higher the frequency of sampling, the stronger the fit. However, there is no evidence that different models could be selected depending on the sampling frequency. In the present study, raw data have been interpolated using a cubic method and the sampling frequency is 1 day over 3. To ensure results, we have tested different interpolation methods, such as linear or nearest, when rebuilding TM signals. Moreover, other sampling frequencies have been used such as 1 day over 6 and every day. It appears that those two aspects do not significantly affect the model selection. The results remain stable, showing the stability of the approach.

Conclusion and perspectives

TM concentrations were used to define PDF and then to study their adequacy with models, allowing a better description of TM concentration dynamics in the environment. Good knowledge of the statistical distributions that rule TM concentrations in the atmospheric aerosol permits better identifying the emission sources in relation to the seasonal variability of concentrations (e.g., TMs that belong to the lognormal group exhibit temporal variations in their concentrations and should be distinguished from TMs of the gamma group, which are characterized by heterogeneous emission sources). This is particularly important in marine environments that are strongly constrained by atmospheric forcing: Owing to numerous and intense land-based emission sources that affect its pelagic environment, the Ligurian Sea is particularly constrained by Aeolian deposition compared with remote oceanic locations. A frontal zone characterized by rapid horizontal changes of density isolates the offshore Ligurian area from the coast (Lévy et al. 1998). As a result, surface waters in the central Ligurian Sea are sheltered from lateral inputs. Therefore, the atmosphere is taken as the only significant source of TMs to the open Ligurian Sea.

Another important perspective for such improved definitions of PDF may be the evaluation of natural and anthropogenic contributions to TM concentrations in the atmospheric aerosol. Assuming that the measured atmospheric signal results from the convolution of two statistically independent random variables (natural and anthropogenic emissions), the statistical numerical analysis of experimental PDF permits discriminating and assessing these respective contributions, at least when large data sets are available (Migon and Caccia 1990). This is particularly important if one considers that the most widely used tools for such studies are enrichment factors, the reliability of which is sometimes questionable, in particular when they are normalized to so-called average soils or rocks, hence the crucial need to improve our knowledge of statistical models that best fit the distribution of a given TM. Among many others, the present work may be a preliminary step to deconvolution studies.

Acknowledgments This work was partly supported by the Conseil Général des Alpes-Maritimes and the Communauté Nice Côte d'Azur (project AIRMED 06). T. Robin contribution was partly supported by the Swiss National Fund. We thank the French Marine team of the Cap Ferrat naval signal station. We also thank Patrick Chang for language corrections. L. Guidi contribution was partly supported by the Center for Microbial Oceanography, Research and Education (C-MORE; NSF grant EF-0424599) and the Gordon and Betty Moore Foundation.

References

Akaike, H. (1974). New look at statistical-model identification. *IEEE T Automation Contraception, 19*(6), 716–723.

Aleksandrapoulou, V., Eleftheriadis, K., Diapouli, E., Torseth, K., & Lazaridis, M. (2012). Assessing PM_{10} source reduction in urban agglomerations for air quality compliance. *Journal of Environmental Monitoring, 14*, 266–278.

Andral, B., Stanisiere, J. Y., Sauzade, D., Damier, E., Thebault, H., Galgani, F., et al. (2004). Monitoring chemical contamination levels in the Mediterranean based on the use of mussel caging. *Marine Pollution Bulletin, 49*, 704–712.

Anwari, M. A., Tuncel, G., & Ataman, O. Y. (1992). Lead and nickel levels in Black Sea aerosols by ETA-AS. *Internal Journal Environmental Analytical Chemistry, 47*, 227–237.

Barnaba, F., & Gobbi, G. P. (2004). Aerosol seasonal variability over the Mediterranean region and relative impact of maritime, continental and Saharan dust particles over the basin from MODIS data in the year 2001. *Atmospheric Chemistry Physics, 4*, 2367–2391.

Bencala, K. E., & Seinfeld, J. H. (1976). On frequency distributions of air pollutant concentrations. *Atmospheric Environment, 10*(11), 941–950.

Blackwood, L. G. (1991). The quality of mean and variance estimates for normal and lognormal data when the underlying distribution is misspecified. *Journal of Chemometrics, 5*(3), 263–271.

Blackwood, L. G. (1992). The lognormal distribution, environmental data, and radiological monitoring. *Environmental Monitoring and Assessment, 21*(3), 193–210.

Bollhöfer, A., & Rosman, K. J. R. (2001). Isotopic source signatures for atmospheric lead: the Northern Hemisphere. *Geochimica et Cosmochimica Acta, 65*(11), 1727–1740.

Bonnet S, Guieu C (2006) Atmospheric forcing on the annual iron cycle in the western Mediterranean Sea: a 1-year survey. J Geophys Res—Oceans 111(C9):Artn C09010. doi:10.1029/2005jc003213

Caggiano, R., Fiore, S., Lettino, A., Macchiato, M., Sabia, S., & Trippetta, S. (2011). $PM_{2.5}$ measurements in a Mediterranean site: two typical cases. *Atmospheric Research, 102*, 157–166.

Chester, R., Nimmo, M., & Corcoran, P. A. (1997). Rain water aerosol trace metal relationships at Cap Ferrat: a coastal site in the western Mediterranean. *Marine Chemistry, 58*(3–4), 293–312.

Chester, R., Sharples, E. J., Sanders, G. S., & Saydam, A. C. (1984). Saharan dust incursion over the Tyrrhenian Sea. *Atmospheric Environment, 18*(5), 929–935.

Chiffoleau, J. F., Chauvaud, L., Amouroux, D., Barats, A., Dufour, A., Pecheyran, C., et al. (2004). Nickel and vanadium contamination of benthic invertebrates following the "Erika" wreck. *Aquatic Living Resources, 17*(3), 273–280.

Chrysikou, L. P., & Samara, C. A. (2009). Seasonal variation of the size distribution of urban particulate matter and associated organic pollutants in the ambient air. *Atmospheric Environment, 43*(30), 4557–4569. doi:10.1016/j.atmosenv.2009.06.033.

Centre Interprofessionnel Technique d'Etudes de la Pollution Atmosphérique (CITEPA) (2009) Air emissions in France, Mainland France, Substances relative to the contamination by heavy metals. www.citepa.org/missions/nationale/ML/Emissions_FRmt_MLEN.pdf

Duncan BN, Bey I (2004) A modeling study of the export pathways of pollution from Europe: seasonal and interannual variations (1987–1997). J Geophys Res—Atmos 109(D8):D08301. doi:10.1029/2003jd004079

Fang, G. C., Huang, Y. L., & Huang, J. H. (2010). Study of atmospheric metallic elements pollution in Asia during 2000–2007. *Journal of Hazardous Materials, 180*(1–3), 115–121. doi:10.1016/j.jhazmat.2010.03.120.

Flament, P., Bertho, M. L., Deboudt, K., & Puskaric, E. (1996). Changes in the lead content of atmospheric aerosols above the Eastern Channel between 1982/83 and 1994. *Science of the Total Environment, 192*(2), 193–206.

Georgiadis, T., Fortezza, F., Alberti, L., Strocchi, V., Marani, A., & Dal Bo', G. (1998). Probability density functions of photochemicals over a coastal area of Northern Italy. *Nuovo Cimento C, 21*(1), 75–84.

Georgopoulos, P. G., & Seinfeld, J. H. (1982). Statistical distributions of air pollutant concentrations. *Environmental Science & Technology, 16*(7), A401–A416. doi:10.1021/es00101a002.

Guerzoni, S., Chester, R., Dulac, F., Herut, B., Loye-Pilot, M. D., Measures, C., et al. (1999). The role of atmospheric deposition in the biogeochemistry of the Mediterranean Sea. *Progress Oceanografia, 44*(1–3), 147–190.

Guieu, C., Chester, R., Nimmo, M., Martin, J. M., Guerzoni, S., Nicolas, E., et al. (1997). Atmospheric input of dissolved and particulate metals to the northwestern Mediterranean. *Deep-Sea Research II, 44*(3–4), 655–674.

Heimbürger, L. E., Migon, C., Dufour, A., Chiffoleau, J. F., & Cossa, D. (2010). TM concentrations in the north-western Mediterranean atmospheric aerosol between 1986 and 2008: seasonal patterns and decadal trends. *Science of the Total Environment, 408*(13), 2629–2638. doi:10.1016/j.scitotenv.2010.02.042.

Hope, B. K. (1994). A global biogeochemical budget for vanadium. *Science of the Total Environment, 141*, 1–10. doi:10.1016/0048-9697(94)90012-4.

Kim, K. H., Kang, C. H., Lee, J. H., Choi, K. C., Youn, Y. H., & Hong, S. M. (2006). Investigation of airborne lead concentrations in relation to Asian dust events and air mass transport pathways. *Journal Aerosol Science, 37*(12), 1809–1825. doi:10.1016/j.jaerosci.2006.08.009.

Lévy, M., Memery, L., & Andre, J. M. (1998). Simulation of primary production and export fluxes in the northwestern Mediterranean Sea. *Journal of Marine Research, 56*(1), 197–238.

Lu, H. C. (2003). Comparisons of statistical characteristic of air pollutants in Taiwan by frequency distribution. *Journal of the Air & Waste Management Association (1995), 53*(5), 608–616.

Marticorena, B., & Bergametti, G. (1996). Two-year simulations of seasonal and interannual changes of the Saharan dust emissions. *Geophysical Research Letters, 23*(15), 1921–1924.

Migon, C., Alleman, L., Leblond, N., & Nicolas, E. (1993). Evolution of atmospheric lead over the northwestern Mediterranean between 1986 and 1992. *Atmospheric Environment, 27*(14), 2161–2167.

Migon, C., & Caccia, J. L. (1990). Separation of anthropogenic and natural emissions of particulate heavy-metals in the western Mediterranean atmosphere. *Atmospheric Environment, 24A*(2), 399–405.

Migon, C., Gentili, B., & Journel, B. (2000). Statistical analysis of the concentrations of twelve metals in the Ligurian atmospheric aerosol. *Oceanologica Acta, 23*(1), 37–45.

Migon, C., Robin, T., Dufour, A., & Gentili, B. (2008). Decrease of lead concentrations in the western Mediterranean atmosphere during the last 20 years. *Atmospheric Environment, 42*(4), 815–821. doi:10.1016/j.atmosenv.2007.10.078.

Mijic, Z., Stojic, A., Perišic, M., Rajšic, S., & Tasic, M. (2012). Statistical character and transport pathways of atmospheric aerosols in Belgrade. In: G. Lopez Badilla, B. Valdez, & M. Schorr (Eds.), *Air quality–new perspectives*. InTech Open Science, 11 (pp. 199–226). doi:10.5772/45873.

Morel, B., Yeh, S., & Cifuentes, L. (1999). Statistical distributions for air pollution applied to the study of the particulate problem in Santiago. *Atmospheric Environment, 33*(16), 2575–2585.

Moulin, C., Lambert, C. E., Dulac, F., & Dayan, U. (1997). Control of atmospheric export of dust from North Africa by the North Atlantic Oscillation. *Nature, 387*, 691–694.

Ott, W. R. (1990). A physical explanation of the lognormality of pollutant concentrations. *J Air Waste Management, 40*(10), 1378–1383.

Pacyna, J. M., Pacyna, E. G., & Aas, W. (2009). Changes of emissions and atmospheric deposition of mercury, lead,

and cadmium. *Atmospheric Environment, 43*(1), 117–127. doi:10.1016/j.atmosenv.2008.09.066.

Pirrone, N., Costa, P., & Pacyna, J. M. (1999). Past, current and projected atmospheric emissions of trace elements in the Mediterranean region. *Water Science Technology, 39*, 1–7.

Ridame, C., Guieu, C., & Loÿe-Pilot, M. D. (1999). Trend in total atmospheric deposition fluxes of aluminium, iron, and trace metals in the northwestern Mediterranean over the past decade (1985–1997). *Journal of Geophysical Research, 104*(D23), 30127–30138.

Rumburg, B., Alldredge, R., & Claiborn, C. (2001). Statistical distributions of particulate matter and the error associated with sampling frequency. *Atmospheric Environment, 35*(16), 2907–2920.

Salma, I., Maenhaut, W., & Zaray, G. (2002). Comparative study of elemental mass size distributions in urban atmospheric aerosol. *Journal Aerosol Science, 33*(2), 339–356.

Sandroni, V., & Migon, C. (1997). Significance of trace metal medium-range transport in the western Mediterranean. *Science of the Total Environment, 196*(1), 83–89.

Schwarz, G. (1978). Estimating dimension of a model. *The Annals of Statistics, 6*(2), 461–464.

Taylor, J. A., Jakeman, A. J., & Simpson, R. W. (1986). Modeling distributions of air pollutant concentrations: I. Identification of statistical models. *Atmospheric Environment, 20*(9), 1781–1789.

Venkataraman, C., Thomas, S., & Kulkarni, P. (1999). Size distributions of polycyclic aromatic hydrocarbons—gas/particle partitioning to urban aerosols. *Journal of Aerosol Science, 30*(6), 759–770.

Wiesner, M. R., Characklis, G. W., & Brejchova, D. (1998) Metals and colloids in urban runoff. In: H. E Allen, A.W. Garrison, & G.W. Luther III (Eds.), *Metals in the environment* (pp. 23–35). Ann Arbor, MI: Ann Arbor Press.

Xie, R. K., Seip, H. M., Leinum, J. R., Winje, T., & Xiao, J. S. (2005). Chemical characterization of individual particles (PM_{10}) from ambient air in Guiyang City, China. *Science of the Total Environment, 343*, 261–272.